SCIENCE CHINA
Earth Sciences

• REVIEW •

November 2010 Vol.53 No.11: 1565–1581
doi: 10.1007/s11430-010-4056-2

Primary scientific results of Chang'E-1 lunar mission

OUYANG ZiYuan[1,2*], LI ChunLai[1], ZOU YongLiao[1], ZHANG HongBo[1], LÜ Chang[1], LIU JianZhong[1], LIU JianJun[1], ZUO Wei[1], SU Yan[1], WEN WeiBin[1], BIAN Wei[1], ZHAO BaoChang[3], WANG JianYu[4], YANG JianFeng[3], CHANG Jin[5], WANG HuanYu[6], ZHANG XiaoHui[7], WANG ShiJin[7], WANG Min[1], REN Xin[1], MU LingLi[1], KONG DeQing[1], WANG XiaoQian[1], WANG Fang[1], GENG Liang[1], ZHANG ZhouBin[1], ZHENG Lei[1], ZHU XinYing[1], ZHENG YongChun[1], LI JunDuo[1], ZOU XiaoDuan[1], XU Chun[1], SHI ShuoBiao[1], GAO YiFei[1] & GAO GuanNan[1]

[1] *National Astronomical Observatories, Chinese Academy of Sciences, Beijing 100012, China;*
[2] *Institute of Geochemistry, Chinese Academy of Sciences, Guiyang 550002, China;*
[3] *Xi'an Institute of Optics and Precision Mechanics, Chinese Academy of Sciences, Xi'an 710119, China;*
[4] *Shanghai Institute of Technical Physics, Chinese Academy of Sciences, Shanghai 200083, China;*
[5] *Purple Mountain Observatory, Chinese Academy of Sciences, Nanjing 210008, China;*
[6] *Institute of High Energy Physics, Chinese Academy of Sciences, Beijing 100049, China;*
[7] *Center for Space Science and Applied Research, Chinese Academy of Sciences, Beijing 100190, China*

Received March 10, 2010; accepted June 22, 2010

The strategic plan for the development of the unmanned Chinese Lunar Exploration Program is characterized by three distinct stages: "orbiting around", "landing on" and "returning from" the Moon. The first Chinese lunar probe, Chang'E-1, which was successfully launched on October 24th, 2007 at Xichang Satellite Launch Center, and guided to crash on the Moon on March 1st, 2009, at 52.36°E, 1.50°S, in the north of Mare Fecunditatis, is the first step towards the "orbiting around" stage. The Chang'E-1 mission lasted 495 days, exceeding the expected life-span by about four months. A total of 1.37 TB raw data was received from Chang'E-1. It was then processed into 4 TB scientific data products at various levels. Many scientific results have been obtained by analyzing these data, including especially the "global lunar image from the first Chinese lunar exploration mission". All scientific goals of Chang'E-1 have been achieved. It provides much useful materials for further advances of lunar sciences and planetary chemistry. Meanwhile, these results will serve as a firm basis for future Chinese lunar missions.

lunar orbiter, Chang'E-1, scientific data, results

Citation: Ouyang Z Y, Li C L, Zou Y L, et al. Primary scientific results of Chang'E-1 lunar mission. Sci China Earth Sci, 2010, 53: 1565–1581, doi: 10.1007/s11430-010-4056-2

1 Introduction

1.1 China's lunar orbiting project

China's Lunar Exploration Program (CLEP) was also known as the Chang'E Program, named after a famous goddess in Chinese mythology who ascended from Earth and lived on the Moon as a celestial being after drinking an elixir.

The first stage of CLEP, lunar orbiting project, was approved by Chinese government and officially signed-off by Premier Wen Jiabao on January 23rd, 2004. The five sys-

*Corresponding author (email: ouyangzy@nao.cas.cn)

© Science China Press and Springer-Verlag Berlin Heidelberg 2010

tems of CLEP, which include the launch vehicle system, orbiter system, telemetry tracking and command (TT & C) system, launch site system, and ground segment for data, science, and application (GSDSA), were established in April, 2004.

CLEP satellite platform and scientific instruments were assembled in 2005–2006. Meanwhile, two deep space ground stations were constructed. Numerous tests and experiments were carried out simultaneously.

The first Chinese lunar probe, Chang'E-1 was launched on October 24th, 2007, marking China's first step in lunar exploration, and a milestone in China's aerospace industry after Earth satellites and manned spaceflight.

1.2 Operations and maneuver of Chang'E-1 lunar orbiter

Chang'E-1 blasted off on a Long March 3A carrier rocket at 6:05 p.m. (10:05 GMT) on October 24th, 2007, from the No. 3 launching tower at the Xichang Satellite Launch Center in Southwest China.

After launch, Chang'E-1 lunar probe had followed a trajectory that consisted of a sequence of active phase orbits, phasing orbits, lunar transfer orbit, and circumlunar orbits (Figure 1). It took 13 days 14 hours 19 minutes in Chang'E-1's journey from the Earth to the Moon. The flight distance is 2,090,000 km.

Chang'E-1 CCD camera was first powered on November 20th, 2007. The scientific data from Chang'E-1 were received by Beijing and Kunming ground stations simultaneously. The first image from Chang'E-1 was released on December 26th, 2007. One year later, the first version of global map of the Moon was released on December 12th, 2008.

Chang'E-1 was guided to crash on the lunar surface and ended its mission at 08:13:10 UTC, on March 1st, 2009. Impact point was located at 52.36°E, 1.50°S, in the north of Mare Fecunditatis.

2 Scientific goals and instruments

There are four scientific goals of Chang'E-1 lunar probe [1, 2].

The first goal is to map the entire Moon with global 3D stereo images of the Moon. These 3D stereo images are essential materials to study the surface features of the Moon. Using these data, the basic landscape, geological units of the lunar surface, and tectonic maps of the Moon could be outlined. The information can also provide reference for site selection of China's future soft-landing on the Moon.

The second goal is to explore the abundance of key elements on lunar surface, such as K, Th, U, O, Si, M g, A1, Ca, Te, Ti, Na, Mn, Cr, La. One set of Sagnac-based interferometer spectrometer, one set of gamma-ray spectrometer and one set of X-ray spectrometer are designed and served for this purpose. These results could be used to evaluate the amount of important resources of the Moon.

The third goal is to measure the microwave brightness temperature (TB) of the Moon. Combined with information

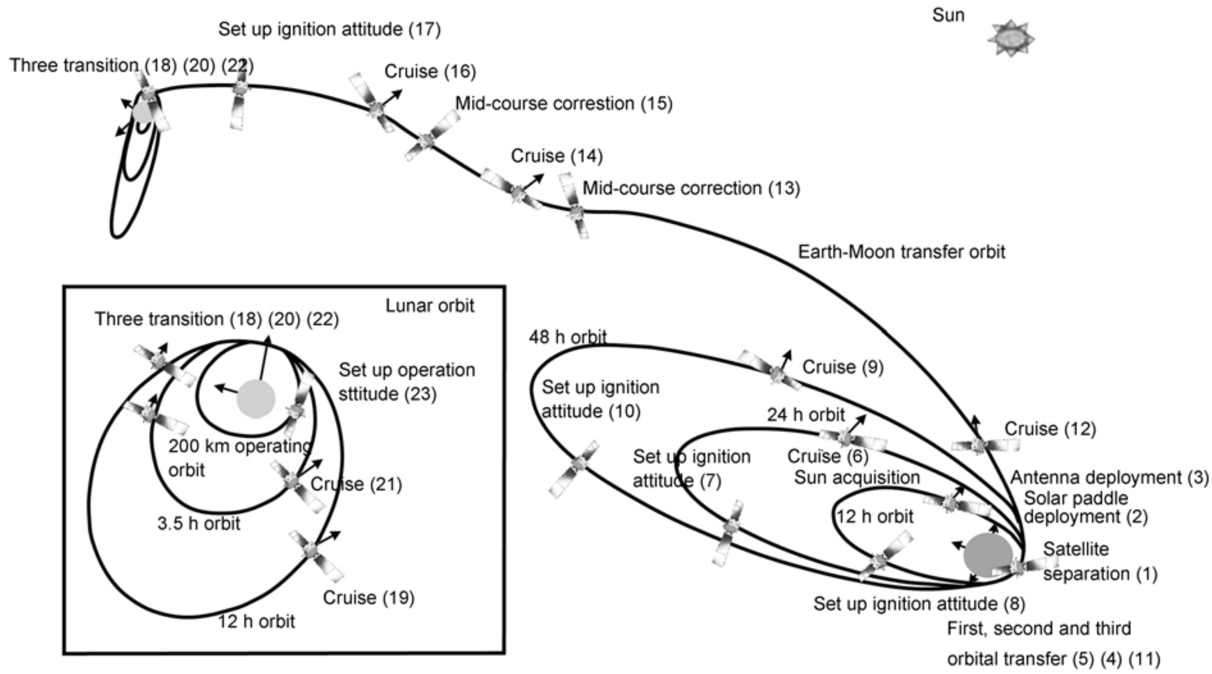

Figure 1 Operations and maneuver of Chang'E-1 lunar orbiter.

about lunar surface composition, TB of the Moon could be used to deduce physical properties and thickness of lunar regolith. Furthermore, the abundance of helium-3 resource can be evaluated. A multi-channel microwave radiometer is designed for this purpose.

The forth goal is to investigate the space environment around the Moon, including the temporal and spatial variations on the composition, intensity, and energy spectrum of solar wind. These data could be used to study the impact of solar activity on the earth and the Moon. A set of high-energy particle detector and two sets of solar wind ion detectors are designed for this purpose.

3 Scientific instruments

To achieve the four mission objectives above, eight sets of scientific instruments are chosen as payloads of CE-1 lunar orbiter, including CCD stereo camera (CCD), Sagnac-based Interferometer Spectrometer (IIM), Laser Altimeter (LAM), Microwave Radiometer (MRM), Gamma-Ray Spectrometer (GRS), X-Ray Spectrometer (XRS), High-energy Particle Detector (HPD), and Solar Wind Ion Detectors (SWID) (Table 1) [1].

4 Scientific data of Chang'E-1

During its 495 days' lifespan, the eight sets of payload aboard Chang'E-1 probe transmitted 1,400 gigabits (GB) of raw data to the ground station. GSDSA has processed and produced 4,000 gigabits (GB) scientific data at various levels (Table 2). The definitions of data at various levels are shown in Table 3. The level 2 and level 3 scientific data have been released to scientists.

5 Primary scientific results from Chang'E-1 data

Primary scientific results from Chang'E-1 data were concluded as follows.

5.1 Obtain three-dimensional stereoscopic image of the Moon

From November 20th, 2007, to July 1st, 2008, the CCD camera successfully mapped the whole surface of the Moon, including the polar areas, where the solar illumination is quite weak. In general, orbital image data are distinctly affected by altitude, solar elevation angle, incidence angle, view angle, exposure time and so on. Data preprocessing algorithms are applied to eliminate these variations in order to produce comparable data in the same situation. Additional image preprocessing procedures, including radiometric calibration, geometric and photometric correction were applied to yield tracks of radiance image data. Finally, standard procedures of Image Map-making, such as Projecting, Geometric positioning and Mosaicing, and Cartographic editingwere applied to smoothly join all tracks of images and created a single global map. A total of 589 tracks of image data, most of which are in vertical view angle, have been used to make a global map of the Moon.

(1) The first lunar image from CE-1 is a composition of images from 19 orbits data acquired on November 20th and November 21st, 2007, and was released on November 26th, 2007 (Figure 2).

(2) The three two-dimensional images, obtained by Chang'E-1 lunar probe, were processed into a three-dimensional image at the same time and released On November 26th, 2007 (Figure 3).

(3) We have also produced 2D and 3D topographic maps of some prominent lunar geologic regions, such as major mares, mounts, lacus, sinus, vallis, rimas, Crater Tycho, and craters named after Chinese persons Chang-Ngo (also spelled as Chang'E), Chang Heng, Wan-Hoo, and Kuo Shou Ching, with CCD camera data.

(4) The Laser Altimeter (LAM) provided 9.16 million range measurements to the lunar surface during its lifespan. These ranges, with accuracy of 100 m and cross-track spacing of 80 km, depict the global shape of the Moon in its center-of-mass frame. Pointing accuracy is a few tenths of a degree, leading to positioning error of many kilometers.

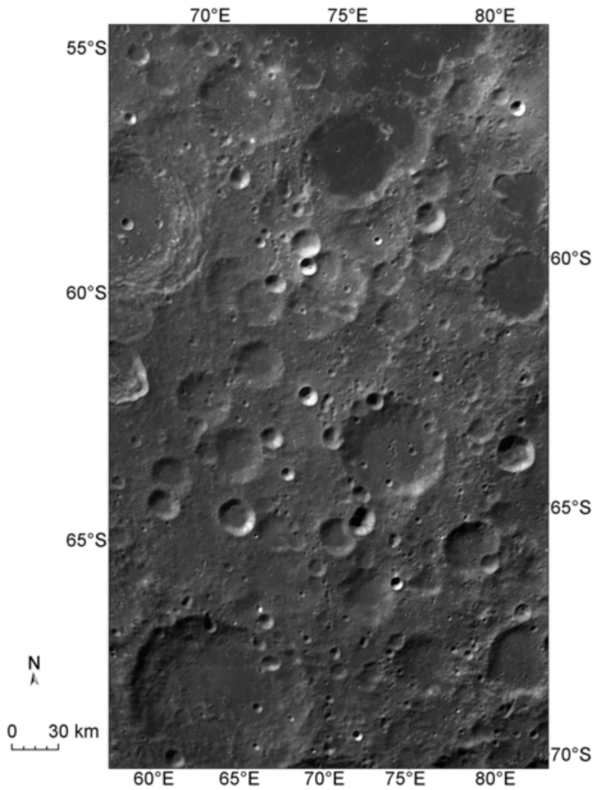

Figure 2 The first lunar image obtained by Chang'E-1 lunar probe.

Table 1 Eight sets of scientific instruments aboard Chang'E-1 lunar orbiter

Scientific goals	Scientific instruments	Principles	Technical indexes
To obtain three-dimensional stereoscopic image of the Moon	Three-line array CCD stereo camera	The Chang'E-1 CCD stereo camera was designed to get three planar images for the same object from three different view angles (forward, nadir and backward), which makes it possible to get DEM data and orthophoto image data of the whole lunar surface.	Spectral range: 500–750 nm Optical channel: 1 Swath width: 60 km Base-height ratio: $\geqslant$0.6 Imaging region: 70°N–70°S Pixel spatial resolution (sub-satellite point): 120 m
	Laser altimeter	Laser pulses were transmitted from Chang'E-1 laser altimeter to the lunar surface. The range from the orbiter to lunar surface is determined by measuring the time delay between transmission of a laser pulse and detection of the back scattered signal from the lunar surface. The altitude of the lunar surface could be calculated from the distance between the spacecraft and the nadir point of the lunar surface.	Range of distance measurement: 200±25 km Footprint on the lunar surface: $\leqslant\Phi$200 m Laser wavelength: 1064 nm Laser energy: 150 mJ Laser pulse width: 5–7 ns Repetition rate of laser pulse: 1 Hz Aperture of reception telescope: 140 mm Focal length of reception telescope: 538 mm Range resolution: 1 m Ranging error: 5 m
To derive the chemical and mineral compositions of the lunar surface materials	Sagnac-based interferometer spectrometer	The Sagnac-based interferometer spectrometer was designed to obtain the multi-spectral image of the lunar surface. Then the composition of lunar surface materials could be derived.	Swath width: 25.6 km Pixel spatial resolution (sub-satellite point): 200 m Imaging region: 70°N–70°S Spectral range: 0.48–0.96 μm Optical channel: 32 Pixel numbers: 256×256 (after 2 pixel×2 pixel combination) S/N: $\geqslant$100
	Gamma-ray spectrometer	To map the elemental abundances of the lunar surface. The gamma-ray spectrometer was designed to measure the gamma-ray photons transmitted from the lunar surface materials. Then the abundance and distribution of some major elements could be derived.	CsI crystal of main detector: Φ118×78 mm Anticoincidence crystal: 30 mm bottom-thickness, 30 mm side thickness Energy resolution of gamma-ray spectrometer: 9%^{137}Cs@662 keV Energy range: 300 keV–9 MeV Number of energy bands: 512 or 1024
	X-ray spectrometer	The X-ray spectrometer was designed to measure the energy spectrum of fluorescence X-rays transmitted from the lunar surface, which is excited by cosmic ray.	Effective area of the probe: 17 cm^2 Energy range: 1–60 keV Resolution: $\leqslant$10%@59.5 keV (Hard X-ray), $\leqslant$600 eV@5.95 keV (soft X-ray) Intrinsic resolution on the lunar surface: 170 km × 170 km (for orbit altitude 200 km) Energy range of solar monitor: 1–10 keV Energy resolution of solar monitor: $\leqslant$600 eV@5.95 keV
To retrieve physical properties and thickness of lunar regolith layers	Microwave radiometer	The microwave radiometer is designed to measure the microwave brightness temperature of the lunar surface. The physical properties and thickness of lunar regolith layer could be derived from. Furthermore, we can estimate quantity and distribution of helium-3 resource on the Moon.	Frequency channels: 3.0 (±1%) GHz, 7.8 (±1%) GHz, 19.35 (±1%) GHz, and 37 (±1%) GHz Integration time: 200 (±15%) ms Brightness temperature sensitivity: $\leqslant$0.5 K Linearity: $\geqslant$0.99
To probe the space environment around the Moon	High-energy particle detector	The high-energy particle detector was designed to measure the energy and flux of heavy ions and protons around the Moon.	Electrons: two energy level (E1: $\geqslant$0.095 MeV; E2: $\geqslant$2.2 MeV) Protons: six energy level (P1: 4–8 MeV; P2: 8–15 MeV; P3: 15–32 MeV; P4: 32–70 MeV; P5: 70160 MeV; P6: 160–400 MeV)
	Solar wind ions detectors	The solar wind ions detectors were designed to detect the composition and distribution of low-energy ions in the solar wind around the Moon. The characteristic parameters of quiet solar wind and high speed solar wind could be retrieved.	Energy range: 0.05–20 keV Number of energy bands: 48 Velocity of solar wind: 150~2000 km/s Instantaneous field of view: 6.7°×180° Acceptance angle: 6.7°×15°

Figures 4 and 5 are global topography maps of the Moon, which are derived from CE-1 Laser Altimeter.

(5) A total of 589 tracks of image data, most of which is in vertical view angle, have been used to make a global map of the Moon (Figure 6). The global image of the Moon was released on November 12th, 2008 [3].

(6) Using 500 m spatial resolution DEM derived from CCD image, we also have developed 3D landscape data of some important lunar geologic units. The following is a 3D map with typical central peak (Figure 7) [4].

(7) We are still producing and developing the global 3D map, diameter and distribution map of craters, and tectonic

Table 2 Amount of scientific data of Chang'E-1 at various levels (MB)

Data amount (MB)	CCD	IIM	LAM	GRS	XRS	MRM	HPD	SWID	Total
Raw data									1,389,641
0 level	433,730	692,464	5,766	72,788	45,792	30,272	1,524	97,794	1,380,130
1 level	30,696	201,385	9,845	22,188	19,524	17,206	3,459	30,734	335,037
2 level	78,029	560,332	926	37,318	56,005	1,334	6,335	79,370	819,649
3 level	3,500		2.39	42			108	7,623	11,273
Total	545,955	1,454,181	16,537	132,336	121,321	48,812	11,426	215,521	3,935,730
Data characteristics	Global coverage	Data with 84% coverage of the Moon from 70°N to 70°S	9,120,000 ranging data	88 days' accumulation data	74 days' accumulation data	Eight times global coverage	120 day's accumulation data		

Table 3 Definition of scientific data at various levels

Levels	Data description
Raw data	Raw data are baseband data received from data transmission receiver in the ground stations
Level 0A	Level 0A data were produced after the procedure of frame synchronization, descrambling and decompression. The UTC time was added.
Level 0B	Level 0B data were produced after sequencing, removing duplication, and optimized stitching for level 0A from two ground stations.
Level 1	Level 1 data were produced after format reorganization and physical quantities conversion of level 0B data, and the description about the data was added.
Level 2	Level 2 data were produced after radiometric calibration, geometric correction and photometric correction of level 1 data. Level 2 data can be produced farther into level 2A, 2B and 2C for different sublevel.
Level 3	Level 3 data were produced after deep processing based on the level 2 data.

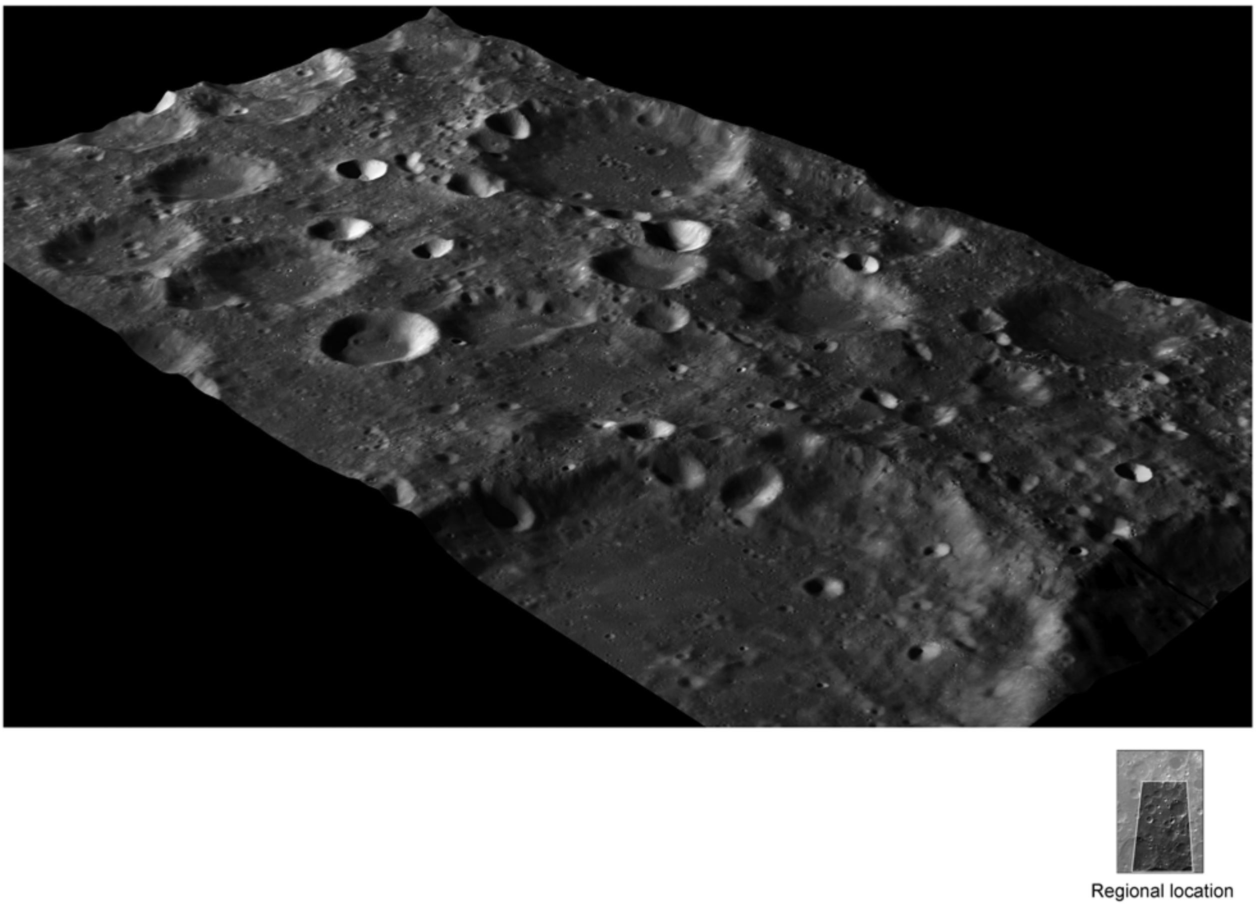

Figure 3 Three-dimensional image obtained by Chang'E-1 lunar probe [4].

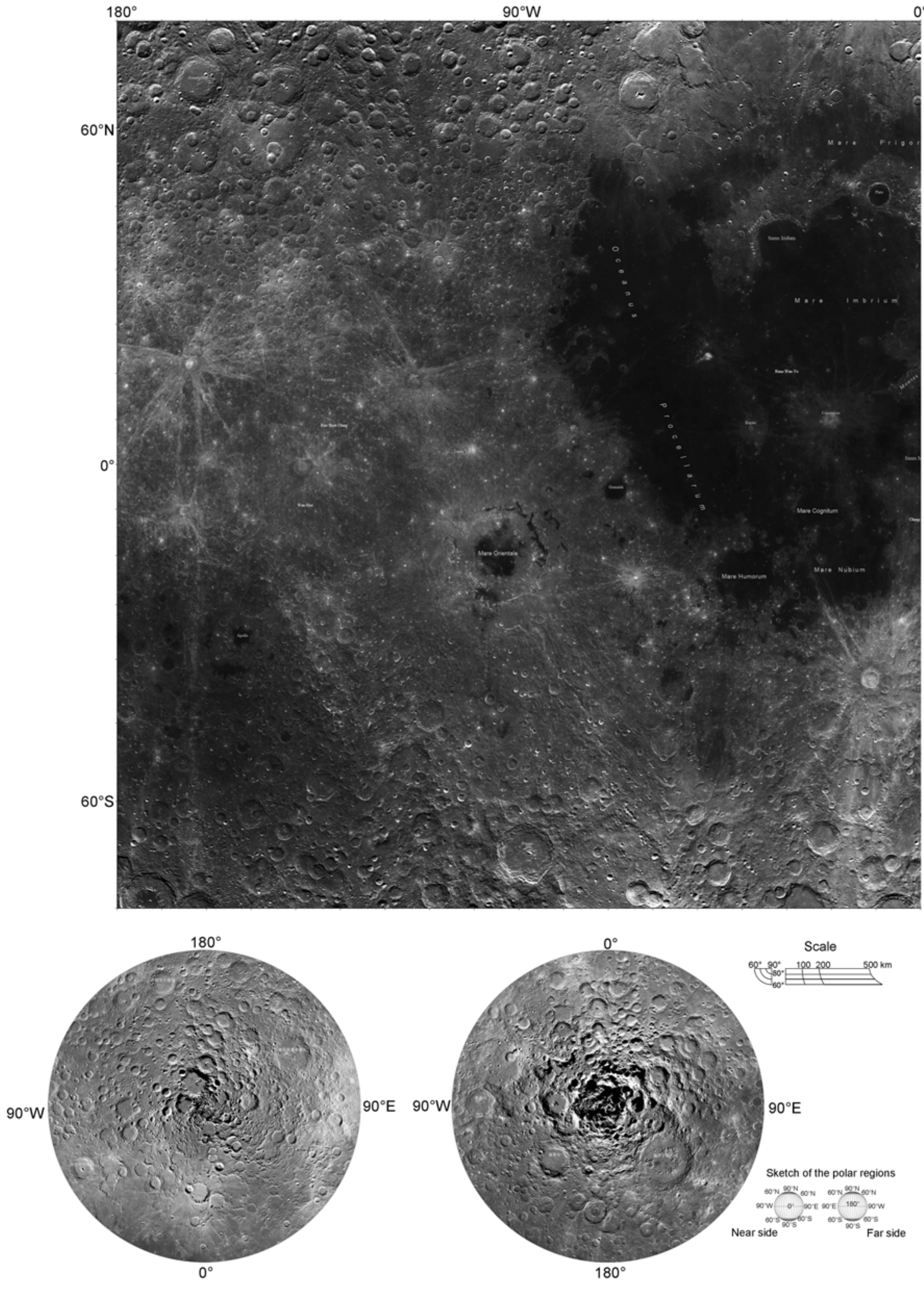
180°
90°W
0°
60°N
0°
60°S
Mare Frigor
Oceanus
Procellarum
Mare Imbrium
Mare Orientale
Mare Cognitum
Mare Humorum
Mare Nubium
180°
90°W
90°E
0°
0°
90°W
90°E
180°
Scale
60° 90° 100 200 500 km
80°
60°
Sketch of the polar regions
Near side
Far side

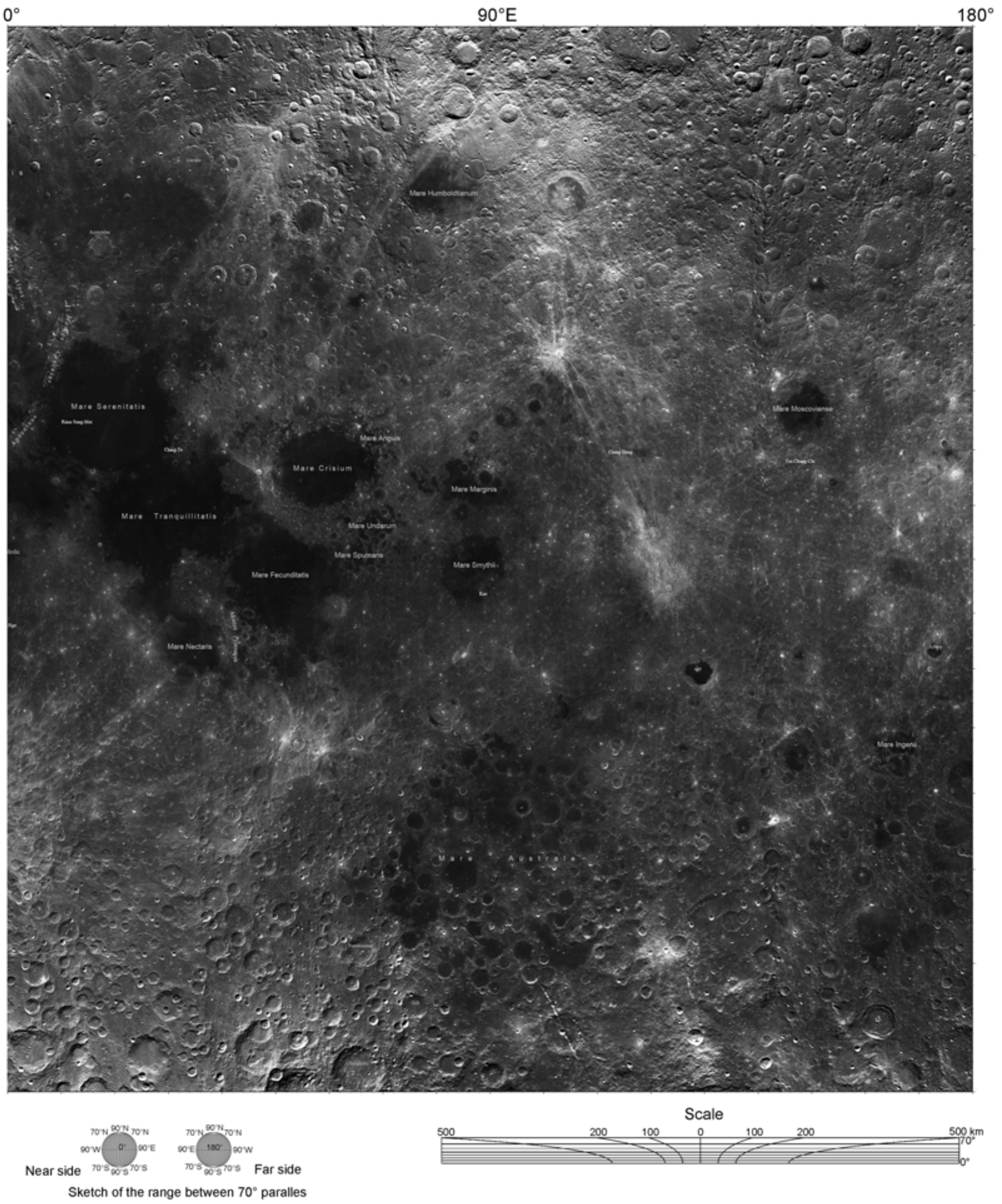

Figure 4 Topography map of the polar region of the Moon by CE-1 laser altimeter. Left, 45°N–90°N; right, 45°S–90°S.

map of linear and circular structures. These maps will be released the subsequently.

5.2 Derive chemical and mineral compositions of the lunar surface

The abundance of elements and distribution of rocks type are important for understanding of the formation and evolution of the Moon. Three sets of payloads on Chang'E-1, i.e., Sagnac-based interferometer spectrometer, gamma-ray spectrometer, and X-ray spectrometer, are selected to detect the distribution of chemical compositions and minerals on the lunar surface. Chang'E-1 IIM images and reflectance properties of Moon, are used to derive the mineralogy, and mineral chemistry of lunar regolith. Gamma-ray spectrometer and X-ray spectrometer data would be used to derive the abundance of some key elements. These payloads were calibrated by our lunar highland [5] and mare [6] soil simulants.

Using inversion model of elemental abundances proposed by Lawrence et al. [7], we have obtained the global abundance maps of radioactive elements U, K, and Th up to October 24th, 2008 (Figures 8 and 9). The abundance and distribution of other elements will be released in the future.

Throughout the normal solar conditions, CE-1 XRS will be able to detect abundance of Mg, Al, and Si in the lunar

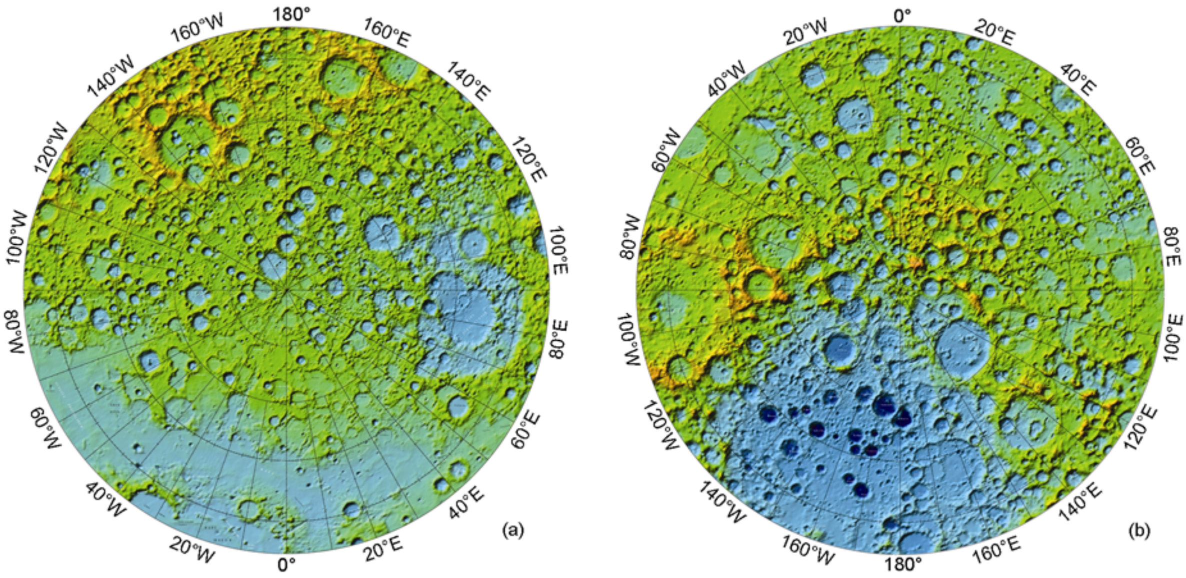

Figure 5 Topography map of the near side (a) and far side (b) of the Moon by CE-1 Laser Altimeter.

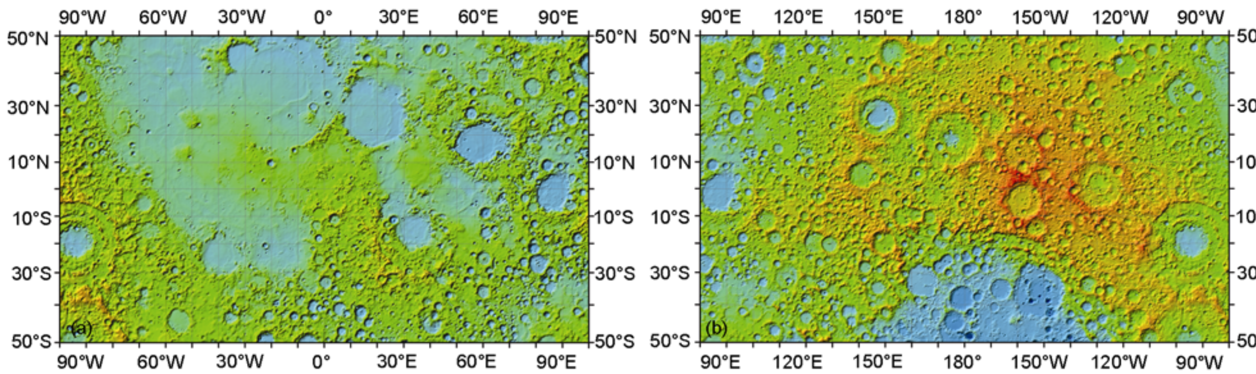

Figure 6 Global lunar image map of China's first lunar mission. (a) Near side; (b) far side.

surface. During solar flare events, it may additionally be possible to detect other elements such as Ca, Ti, and Fe. The X-ray emission from the Moon's surface is excited by solar X-ray photons. Unfortunately, the year 2008 was the solar minimum year in solar cycle of 23 years, which means that the solar X-ray flux was the lowest. Accordingly, the lunar fluorescent X-rays excited by the solar X-rays were so few that the elemental abundance distribution could hardly be determined. The onboard solar monitor has recorded solar X-ray bursts from December 31st, 2007 to January 2nd, 2008, and these data could be used to detect abundance of Mg, Al, and Si within an area of 3×10^6 km^2 on the lunar surface.

CE-1 IIM has completed 84% coverage of the lunar surface between 70°S and 70°N. A series of models have been developed to predict the iron abundance from Clementine UVVIS images. We have developed preliminary algorithms to map FeO and TiO_2 abundance from Chang'E-1 IIM images [8]. Combined with the abundance of some key elements derived from GRS and XRS, the distribution of KREEP rocks, basalt and plagioclase can be outlined.

5.3 Retrieve physical properties and thickness of lunar regolith layers

A set of four channel microwave radiometer (MRM) was boarded on CE-1, which worked at 3.0, 7.8, 19.35, and 37 GHz. Up to now, CE-1 MRM is the first passive microwave remote sensor deployed in all lunar orbiter, which has completed eight times of coverage to measure the microwave radiation from the Moon. The spatial resolution, temperature sensitivity, and coverage of CE-1's brightness temperature (TB) data sets are much better than any other ground-based observation by radio observatories [9]. For wavelength of microwave longer than visible band, microwave radiation can penetrate the loose lunar surface from a few centimeters to several tens of meters. Thus, physical properties of deep layers could be sensed and retrieved from

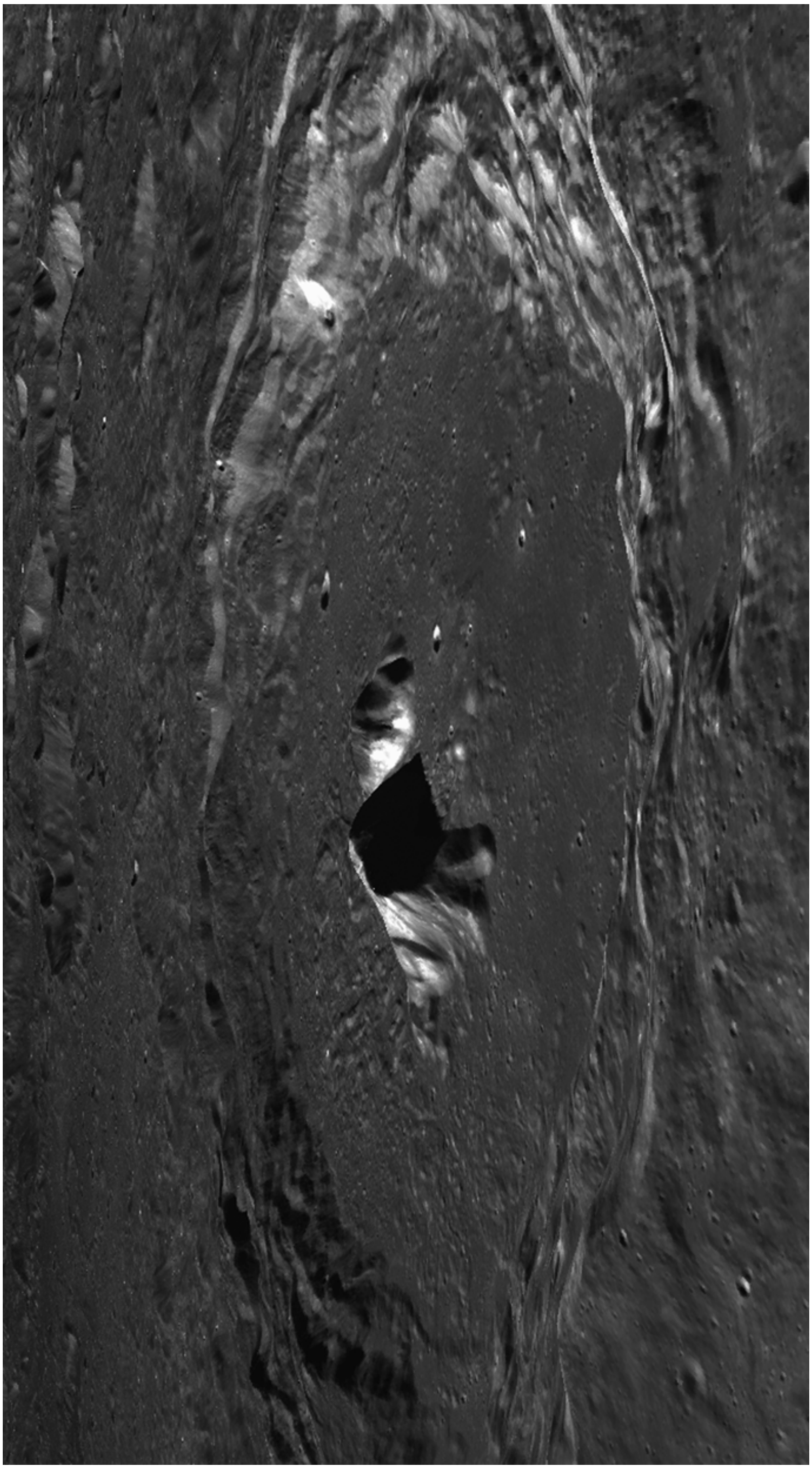

Figure 7 3D map of a crater with typical central peak (spatial resolution is 500 m).

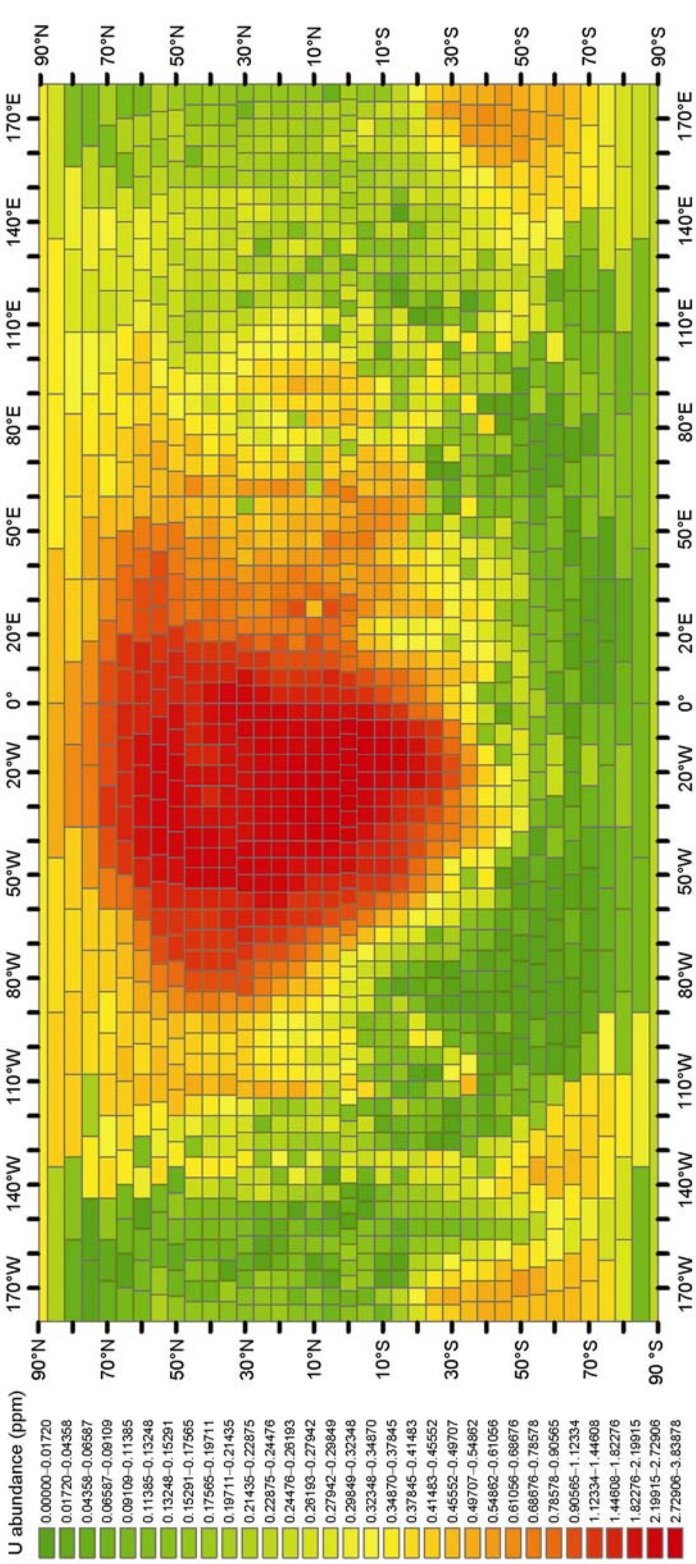

Figure 8 Global map of uranium abundance. A pixel size is square of 5° for longitude and latitude.

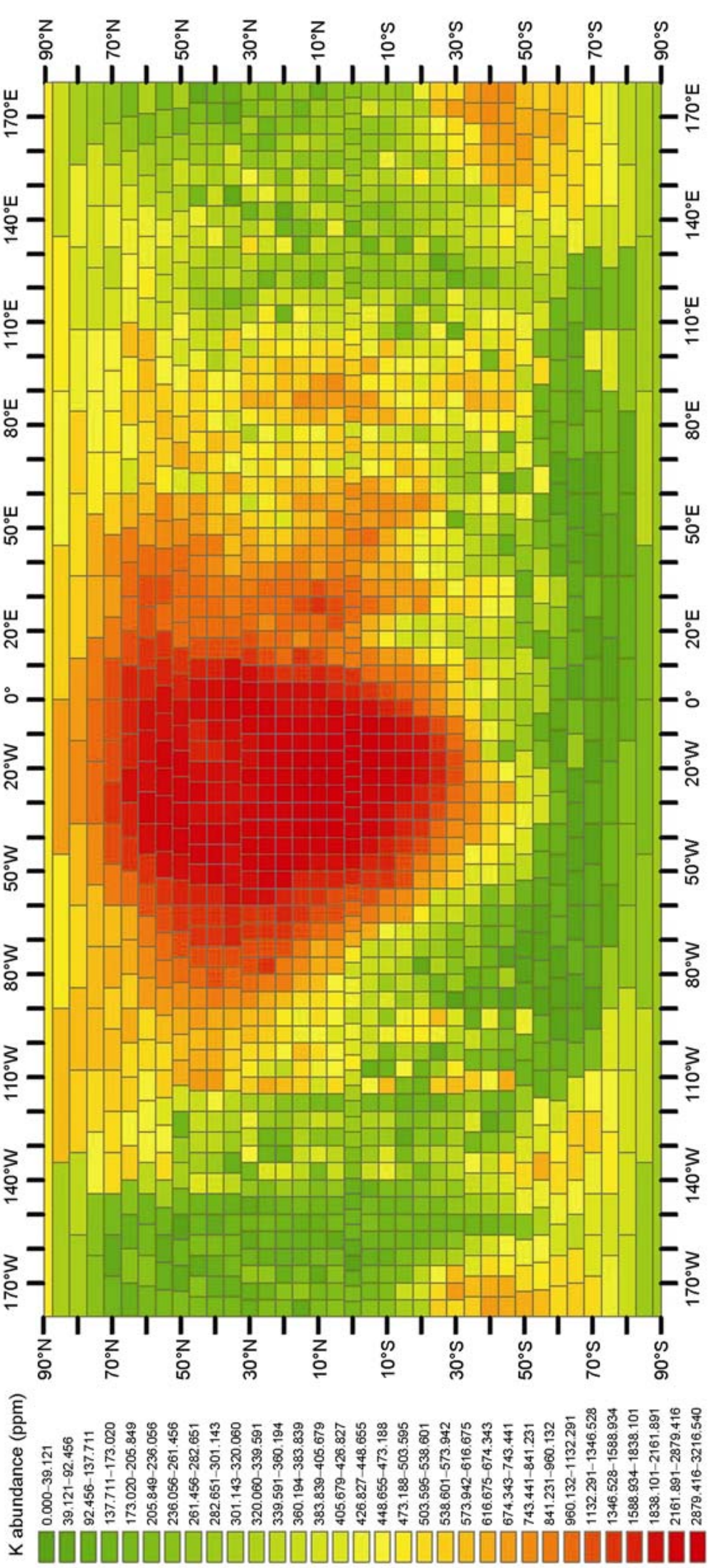

Figure 9 Global map of potassium abundance. A pixel size is square of 5° for longitude and latitude.

TB of the Moon [10].

Brightness temperature of the Moon has been derived by orbital two-point calibration. The radio sources, which could contribute to the cold sky calibrating antenna of CE-1 MRM, have been eliminated. The method and flow data processing were constructed, and the error was estimated. We also have constructed a microwave radiation transfer model of the Moon.

In future work, other factors contributed to TB of the Moon , such as surface roughness, volume scattering effects produced by rock block in the regolith, and layered structure of lunar regolith, will be considered. Microwave radiation transfer model of the Moon should be refined.

Daytime and nighttime TB data of the Moon at frequency of 3.0, 7.8, 19.35, and 37.0 GHz have been mapped (Figures 10 and 11). The Moon maps show that TB in higher latitude zone was lower than that in low latitude. Large craters, boundaries between mare and highland, and basins could be identified easily from the map, which suggests that TB is controlled mainly by lunar topography. Hot regions are seen in dark mare, which is accounted for by higher abundance of titanium-containing mineral ilmenite in the mare. Ilmenite is a lossy material which absorbs more microwave radiations than anorthosite in the highland.

5.4 Probe the space environment around the Moon

A high energy particle detector (HPD) and two solar wind ion detectors (SWIDs) are onboard to explore the space environment in the lunar orbit. During its operation, the spacecraft passed the interplanetary space, the lunar wake, magnetosheath (MS) and magnetotail (MT) of the Earth. Measurements from HPD were rare in the interplanetary space, while it observed electrons of 0.1 MeV in MS and MT (Figure 12).

CE-1's solar wind ions detectors contain more information than HPD (Figure 13). These data reveal several characteristics of geo-space plasma. In the interplanetary space, solar wind plasma exhibits typical characteristics of high density, low temperature, and few disturbances. Plasma temperature and disturbance were enhanced when passing through the magnetic sheath of Earth's geomagnetic field. In the magnetotail, the density is very low, with much higher proton temperature.

SWIDs also observed the dynamics of newly discovered reflected solar wind protons. The acceleration of reflected protons at dayside of lunar surface and the polar terminator region revealed some new details of the kinetic nature of the solar wind interaction with the Moon [11].

5.5 Crashed on the Moon

The velocity of Chang'E-1 was reduced to 1.627 km/s after operations and maneuvers on March 1st, 2009. The CCD camera maintained its operation from 59 km above the lunar surface when CE-1 was aimed at the impact point within Mare Fecunditatis. At 16:13:10, on March 1st, 2009, Chang'E-1 crashed on the lunar surface at 52.36°E, 1.50°S. The CCD camera had recorded the 1469 km images of the lunar surface before the crash (Figure 14).

6 Conclusions and discussion

Through the success of the first Chinese lunar exploration project, a number of key technological breakthrough have been achieved. These include the technologies of CCD image processing, global image map-making, automatic DEM generation from CE-1's CCD stereo camera images, processing of LAM ranging data, and CCD images in combination with LAM data. We also obtained innovative scientific results in the research and application of CE-1 data. These results have been and will be published in journals, conferences, and patents.

The global image map of the Moon has been acquired from CE-1 CCD image. This image map covers the entire lunar surface at an uniform spatial resolution of 120 m. The Chinese global image map of the Moon provides a new, highly precise, and global data for lunar topographic demonstration and research. Because the CCD data are based on views from the CCD stereo camera set of three, they enable us to map the entire Moon in 3D at a very high resolution. The next step is to extract the DEM data using the 3D data by the photogrammetry method. The 1:2500000 global digital relief map with contour interval ≤500 m and 100% coverage will be released in the coming months. Global DEM of the Moon, derived from 9.16 million ranges data of CE-1 laser altimeter, also has been acquired. In the geologic and geographic analysis, and selection of landing sites for the lunar lander and rover, the new image and 3D map will play an important role.

As the first of passive microwave remote sensor in all lunar orbiters, CE-1 MRM has completed eight times of coverage to measure the microwave radiation of the entire Moon. The spatial resolution, temperature sensitivity, and coverage of CE-1's brightness temperature (TB) data sets are much better than any other ground-based observation by radio observatories. The thickness of lunar regolith at some typical regions has also been derived from TB data. Other physical properties of regolith layers could be retrieved in the future. Chang'E-1's TB data sets suggest that the TB of the Moon is controlled obviously by the topography and composition of lunar surface materials.

HPD and SWIDs had accumulated a large amount of data that are rich in physics. From these data we can learn much about space environment characteristics of the Lunar-Terrestrial system. The scientific objective of the monitoring of lunar space environment was completed. As a

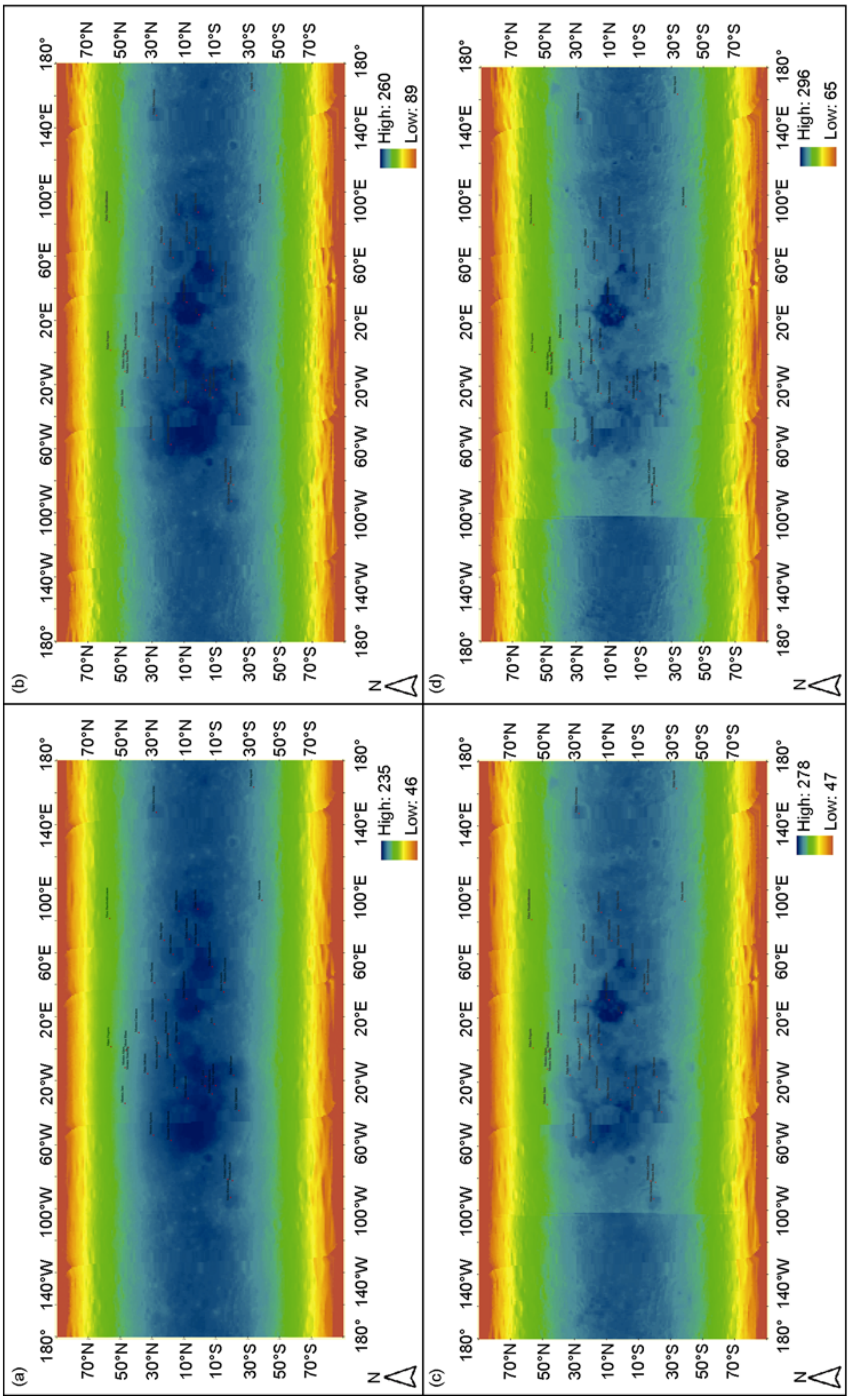

Figure 10   Daytime TB of the Moon at frequency of 3.0 GHz (a), 7.8 GHz (b), 19.35 GHz (c), 37.0 GHz (d).

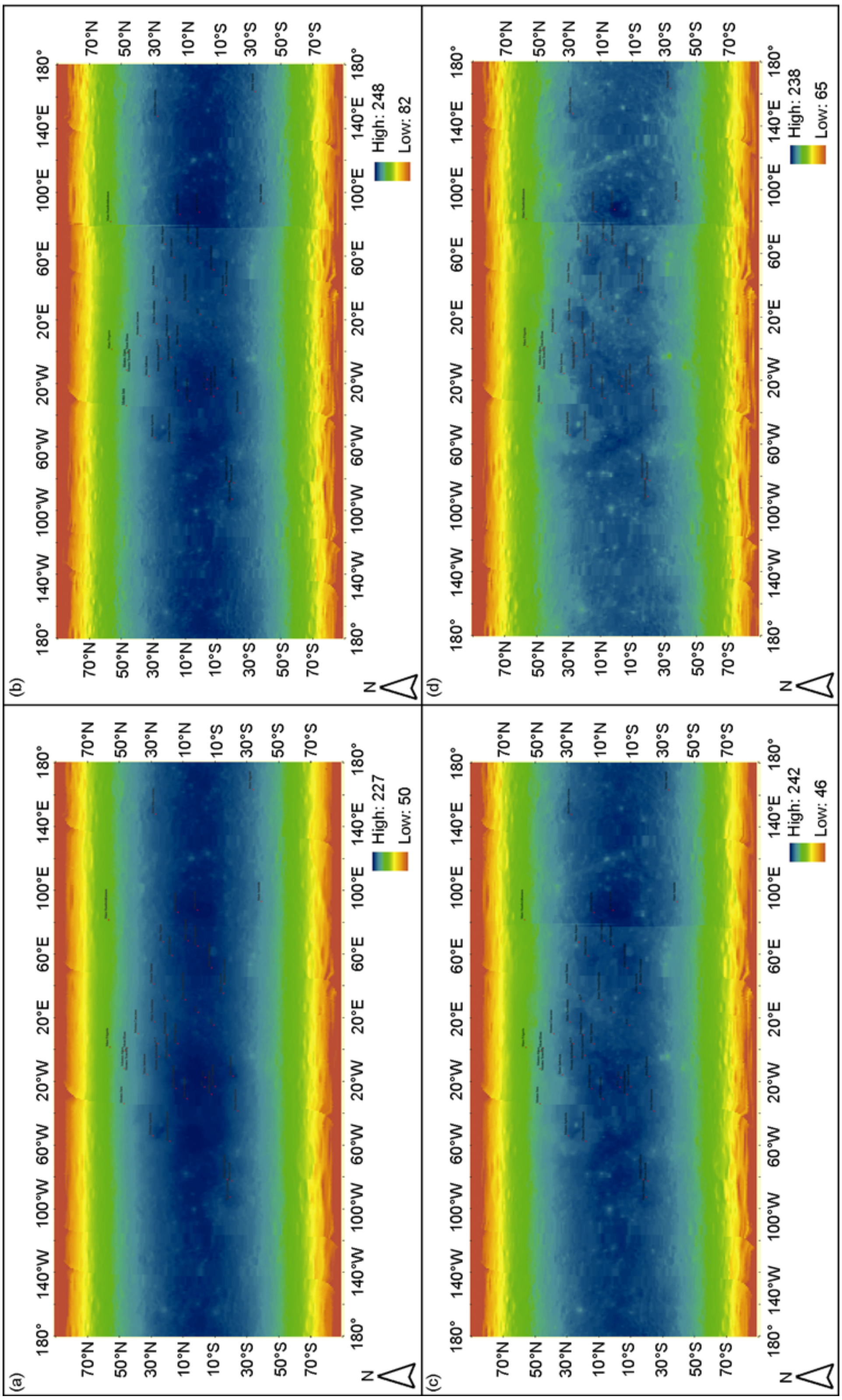

Figure 11 Nighttime TB of the Moon at frequency of 3.0 GHz (a), 7.8 GHz (b), 19.35 GHz (c), 37.0 GHz (d).

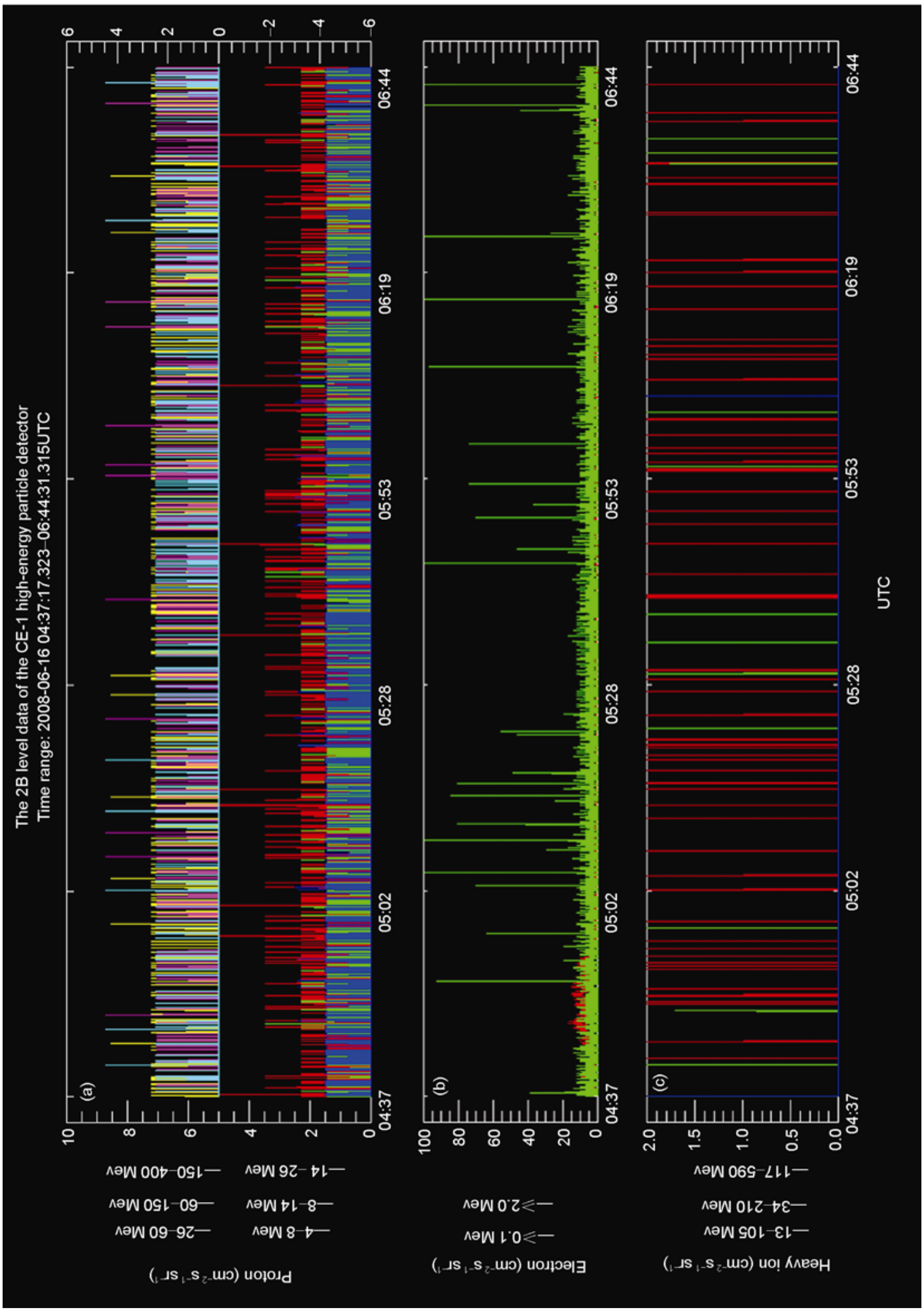

Figure 12 High-energy particle counts of CE-1's HPD in the magnetic sheath (a) and solar wind ions spectra of CE-1's SWIDs ((b), (c)).

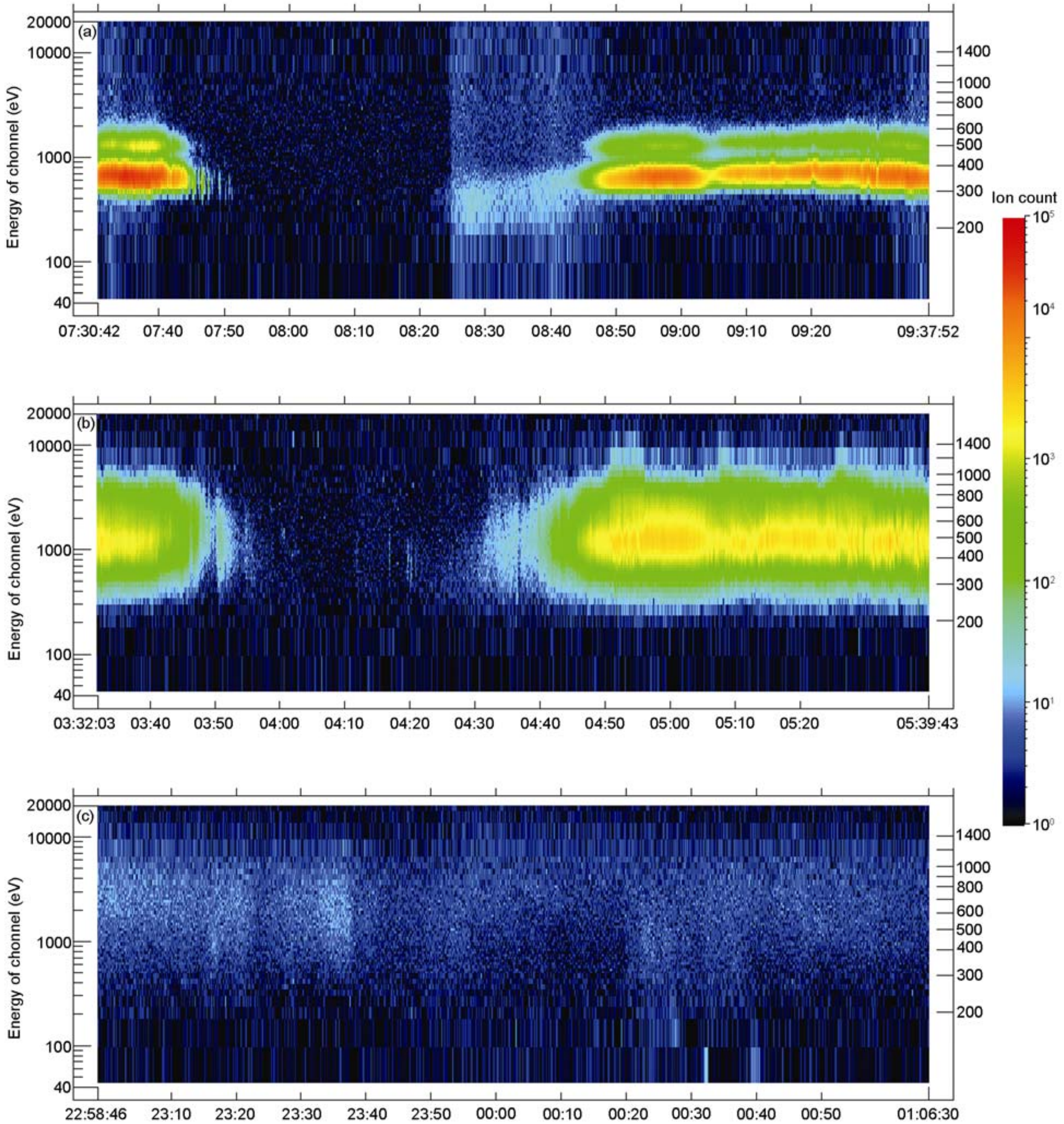

Figure 13 Energy spectrum of solar wind plasma. (a) In the interplanetary space (data from orbit 600); (b) in the magnetic sheath of Earth's geomagnetic field (data from orbit 236); (c) in the magnetotail (data from orbit 539).

weakly magnetized airless obstacle, the Moon interacts with the solar wind directly, producing some unique features. Before the recent three Asian missions including Chang'E-1, the plasma environment close (100–200 km altitude) to the Moon had not been extensively observed.

CE-1's GRS, IIM, and XRS have detected the abundance of some key elements and distribution of minerals on the Moon. Using these results, we can outline the distribution of KREEP rocks, mare basalt, and highland plagioclase. Fine tectonic map will be released based on CE-1 data in the future.

The success of Chang'E-1 is the first step toward deep space exploration for China. Large numbers of data have been acquired from the eight sets of payloads. We also have made beneficial tests in data processing and retrieving algorithms. Some scientific results have been submitted to journals and conferences, and will be published in the near future.

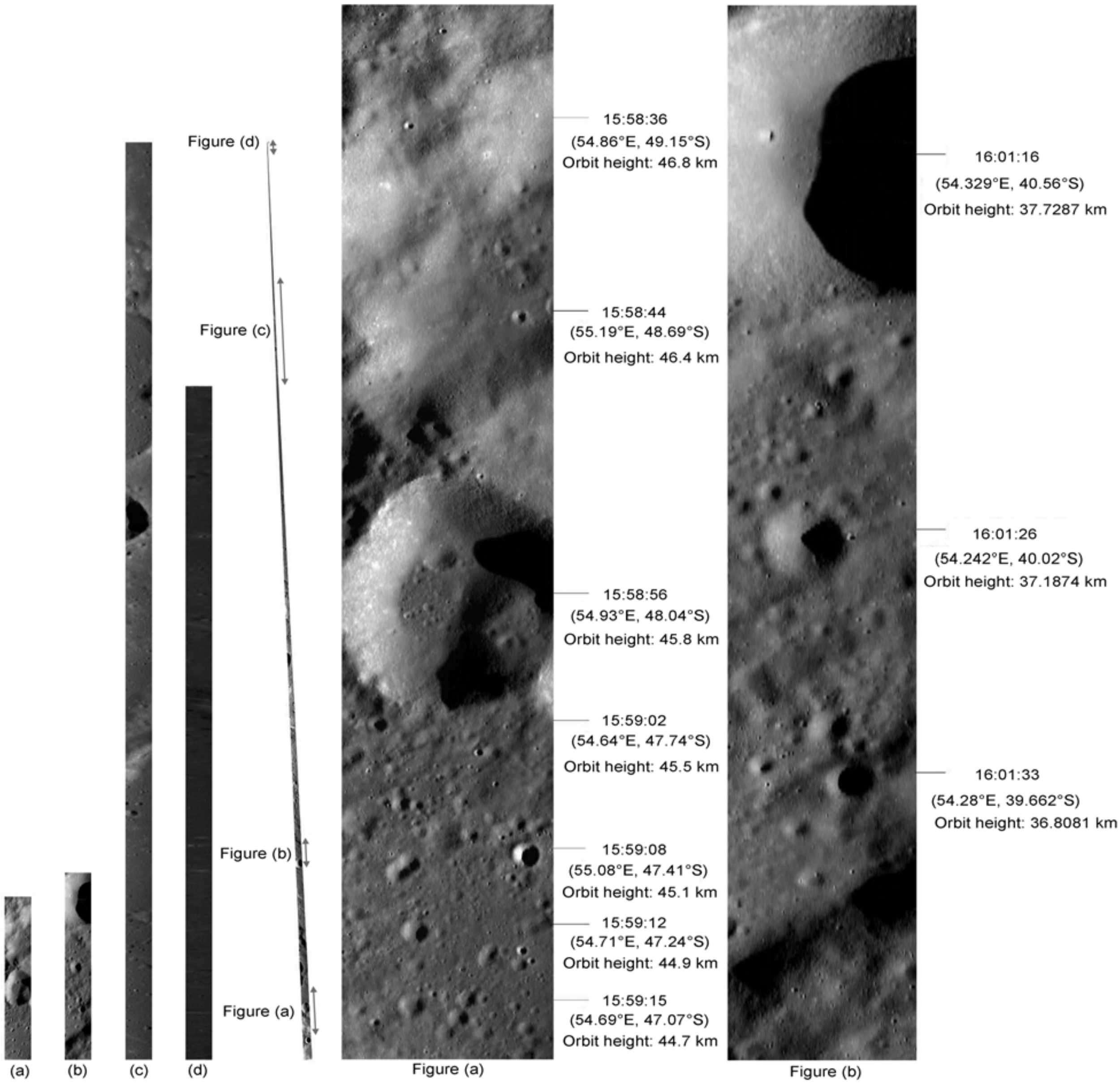

Figure 14 Images of the lunar surface before Chang'E-1 crash.

China's lunar orbiting project is a joint accomplishment under cooperation of China National Space Administration, General Armament Department, Chinese Academy of Sciences, China Aerospace Science and Technology Corporation. In the receiving, processing and application research of Chang'E-1 data, we get help and support from many universities and institutes. We thank all engineers and scientists who contribute to the project.

1 Ouyang Z Y. Introduction to Lunar Science (in Chinese). Beijing: China Astronautic Publishing House, 2005. 362

2 Ouyang Z Y, Jiang J S, Li C L, et al. Preliminary scientific results of Chang'E-1 lunar orbiter. Chin J Space Sci, 2008, 28: 917

3 Li C L, Liu J J, Ren X, et al. The global image of the Moon obtained by the Chang'E-1: Data processing and lunar cartography. Sci China Earth Sci, 2010, 53: 1091–1102

4 Liu J J, Ren X, Mu L L, et al. Automatic DEM Generation from CE-1's CCD Stereo Camera Images. In: 40th Lunar Planetary Science Conference, Texas, 2009. 2570

5 Zheng Y C, Wang S J, Ouyang Z Y, et al. CAS-1 lunar soil simulant. Adv Space Res, 2009, 43: 448–454

6 Li Y Q, Liu J Z, Yue Z Y. NAO-1: A lunar highland soil simulant developed in China. J Aerosp Engrg, 2009, 22: 53–57

7 Lawrence D J, Feldman W C, Barraclough B L, et al. Thorium abundances on the lunar surface. J Geophys Res, 2000, 105(E8): 20307－20331

8 Zheng Y C, Wang S J, Ouyang Z Y. Dielectric properties of lunar material and its microwave penetration depth. Geochim Cosmochim Acta, 2005, 69: A805

9 Chan K L, Tsang K T, Kong B, et al. Lunar regolith thermal behavior revealed by Chang'E-1 microwave brightness temperature data. Earth Planet Sci Lett, 2010, 295: 287–291, doi: 10.1016/j.epsl.2010.04.015

10 Jiang J S, Wang Z Z, Li Y. Study on theory and application of CE-1 microwave sounding lunar surface (in Chinese). Eng Sci, 2008, 10: 16–22

11 Wang X D, Bian W, Wang J S, et al. Acceleration of scattered solar wind protons at the polar terminator of the Moon: Results from Chang'E-1/SWIDs. Geophys Res Lett, 2010, 37: L07203, doi: 10.1029/2010GL042891